Review Article

Thoracic electrical impedance tomography: an adaptive monitor for dynamic organs

Alessandro Santini[1], Elena Spinelli[1], Thomas Langer[1,2], Savino Spadaro[3], Giacomo Grasselli[1,2], Tommaso Mauri[1,2]

[1]Dipartimento di Anestesia, Rianimazione ed Emergenza-Urgenza, Fondazione IRCCS Ca' Granda Ospedale Maggiore Policlinico, Milan, Italy; [2]Dipartimento di Fisiopatologia Medico-Chirurgica e dei Trapianti, Università degli Studi di Milano, Milan, Italy; [3]Dipartimento di Morfologia, Chirurgia e Medicina Sperimentale, Sezione Anestesia e Rianimazione, Università di Ferrara, Ferrara, Italy

Contributions: (I) Conception and design: A Santini, T Mauri; (II) Administrative support: None; (III) Provision of study material or patients: None; (IV) Collection and assembly of data: A Santini, E Spinelli, T Langer, S Spadaro, G Grasselli; (V) Data analysis and interpretation: All authors; (VI) Manuscript writing: All authors; (VII) Final approval of manuscript: All authors.

Correspondence to: Tommaso Mauri, MD. Dipartimento di Anestesia, Rianimazione ed Emergenza-Urgenza, Fondazione IRCCS Ca' Granda Ospedale Maggiore Policlinico, Milan, Italy. Postal address: via Francesco Sforza 28, 20122, Milan, Italy. Email: tommaso.mauri@unimi.it.

Abstract: Electrical impedance tomography (EIT) is increasingly used in intensive care patients to monitor pulmonary and cardiac function non-invasively at the bedside. Impedance variations measured by EIT due to a change in thoracic air content represent the largest and most studied signal, allowing the measurement of end-expiratory lung volume (EELV), global and regional ventilation and spatial and temporal heterogeneity of ventilation distribution. This technique gives a dynamic, repeatable, global and regional description of the respiratory system mechanics, providing at the same time a dynamic picture of lung function. A smaller but detectable change in electrical impedance is due to the increase/decrease of blood content into lung vascular tree during the cardiac cycle. This signal is used to measure stroke volume and global and regional lung perfusion. The integration of the ventilation and perfusion components of the EIT signal can be used to measure ventilation-perfusion matching. The aim of this review is to describe the current clinical applications of EIT, providing a guide to the most relevant physiologic variables derived from EIT and their clinical meaning. We will focus on respiratory and cardiac-related variables and their application in both the anesthetized and awake patients. A special attention will be given to two greatly expanding fields of use: pediatric patients and the perioperative (adult and pediatric) setting. Finally, we will describe potential future applications which we expect will soon become a reality, with the potential to change our everyday practice in the intensive care unit and the operating theatre.

Keywords: Electrical impedance tomography (EIT); critical-illness; lung; hemodynamic monitoring; pediatric

Received: 13 August 2018; Accepted: 20 August 2018; Published: 03 September 2018.
doi: 10.21037/jeccm.2018.08.08
View this article at: http://dx.doi.org/10.21037/jeccm.2018.08.08

Introduction

Since the invention of the stethoscope by Laennec and the performance of the first radiography by Roentgen to his wife's hand, medicine started moving from the observation of the body surface to deep organs investigation. Different technologies have been developed to help clinicians understand anatomy (e.g., CT scan) and (patho)physiology (e.g., airway pressure and flow measurement), but hardly any single measure links the two. Anatomical images show a static, detailed picture of the lungs with high spatial but no temporal resolution, while functional tests give a global indication of performance, with no possibility to dissect regional contributions.

More recently, an anatomical and functional bedside monitoring technique, electrical impedance tomography

© Journal of Emergency and Critical Care Medicine. All rights reserved.

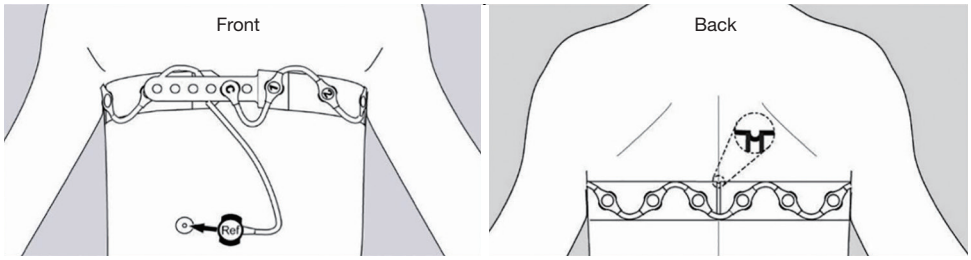

Figure 1 Belt position for EIT monitoring. EIT belt positioning at the fifth intercostal space in a standard patient, front (left panel) and back (right panel) view. Position of the belt and the reference electrode is shown. The belt can be adjusted to patient's chest dimensions and centered using the vertebral spinous processes as markers. EIT, electrical impedance tomography.

(EIT), has been introduced in clinical practice. EIT allows dynamic, repeatable, global and regional description of lung function; its non-invasiveness and portability makes it an ideal monitoring tool in both awake, spontaneously breathing subjects and in anesthetized, intubated critically-ill patients.

In this review, we will highlight the advantages of EIT over conventional tests, describe its principle of functioning, current clinical use and potential applications in both adults and pediatric patients.

Principles of function

EIT requires the placement of standard electrodes on the chest circumference, usually at the 5^{th}–6^{th} intercostal space. Commercially available EIT devices now integrate 16 or 32 equally spaced electrodes into belts or stripes. The belt is typically placed in one transverse plane (*Figure 1*), although oblique placement has also been described. To generate functional EIT images, very small alternating electrical currents are applied through pairs of electrodes, while the remaining ones measure the resulting voltages. Current application and voltage measurement is through adjacent electrode pairs, then sequentially spinning around the belt at 10–50 Hz frequency (1). The set of EIT data acquired during one cycle of current application and voltage measurements is used to generate a single raw EIT image. A sequence of EIT images dynamically map the regional changes over time of the electrical tissue resistance to alternate currents (i.e., impedance) of a slice of the thorax with a cranium-caudal thickness of about half the lungs size. Specifically, an increase in regional gas content increases impedance because it lengthens the path the applied electrical current must follow, while an increase in blood or fluid volume decreases impedance. The magnitude of the impedance changes generated by tidal ventilation is higher and slower than the changes induced by heart activity and lung perfusion, thus making ventilation monitoring far more advanced than assessment of central hemodynamics. To increase the sensitivity of EIT data analysis, only waveforms originating from specific regions of interest (ROIs) should be analyzed (e.g., the lungs for ventilation and perfusion or the heart for cardiac output) but the border between the pulmonary and non-pulmonary tissue is not clearly defined in EIT images. Anyway, ROI-based analysis of EIT is helpful to dynamically characterize the spatial heterogeneity of lung ventilation and perfusion (i.e., two measures that are unique to this monitoring system); this requires the application of arbitrary ROIs, such as gravitationally-oriented same-size layers.

Measured and derived variables

A very high number of variables can be derived by EIT monitoring, potentially making the interpretation of study results confusing (*Table 1*). Below, we suggest a few macro-categories to guide clinicians and researchers approaching EIT for the first time. EIT variables usually fall within the following:

(I) Quantification of global and regional ventilation: changes of chest impedance are linearly correlated with tidal ventilation, both at the global and regional level (2). In this way, tidal ventilation can be assessed in patients lacking spirometry monitoring (e.g., non-intubated patients), while pixel-level ventilation might be used to monitor the changes in hypo-ventilated units (i.e., silent spaces) induced by alveolar recruitment (3);

(II) Spatial heterogeneity of ventilation distribution: inhomogeneous distribution of lung ventilation

© Journal of Emergency and Critical Care Medicine. All rights reserved.

Table 1 EIT-derived variables

Unit of measure	Spatial resolution	Variable of interest	Time resolution	Derived variables	Clinical use
Z	Global	Volume	End-expiration	End-expiratory lung volume	Changes over time (recruitment/ derecruitment)
Z	ROI	Volume	End-expiration	End-expiratory regional volume	Recruitment Dynamic hyperinflation
ΔZ/ΔPaw	Global or ROI	Ventilation	Tidal cycle	Compliance	Changes over time (recruitment/ derecruitment)
ΔZ	ROI	Ventilation	Tidal cycle	Re-ventilation	Re-expansion of a previously collapsed area
ΔZ	ROI or pixel	Air movement	Start of inspiration	Pendelluft	Unassisted breath
ΔZ	ROI or pixel	Air movement	End-inspiration	Pendelluft	Time constant inequalities
ΔZ%[†]	ROI	Ventilation	During inspiration	Heterogeneity of ventilation	Intratidal recruitment or overdistention
ΔZ non-dep/dep	ROI	Ventilation	Tidal cycle	Heterogeneity of ventilation	Maldistribution of ventilation, stress risers
Cardiac ΔZ	Global	Hemodynamics	Cardiac cycle	Stroke volume	Non-invasive cardiac output measurement
Cardiac ΔZ	Global	Hemodynamics	During tidal ventilation	Stroke volume variation	Fluid responsiveness
Cardiac ΔZ	ROI	Perfusion	Cardiac cycle	Blood flow	Regional lung perfusion
ΔZ/Cardiac ΔZ	ROI	Ventilation/ Perfusion	Tidal/cardiac cycle	Shunt and dead space	Pulmonary embolism, atelectasis/alveolar flooding

EIT-derived variables most often reported in the literature to describe cardio-pulmonary function are reported, along with the timeframe in which they are measured and their clinical meaning. [†], ΔZ% is commonly referred to as "intratidal ventilation distribution" (ITV). Z, impedance; ROI, region of interest; Paw, airway pressure; non-dep, non-gravitationally dependent; dep, gravitationally dependent; EIT, electrical impedance tomography.

causes local multiplication of transpulmonary pressure (4). Thus, EIT-based protective ventilation strategies could be based on improvement of the various inhomogeneity indexes [e.g., global inhomogeneity (GI) index or center of ventilation (5)];

(III) Regional respiratory system mechanics: if regional tidal ventilation is divided by driving pressure, regional compliance can be calculated. Improved compliance can then be used to detect decreased alveolar over-distension or recruitment (6);

(IV) Quantification of global and regional change of the end-expiratory lung volume (EELV): changes in end-expiratory impedance are correlated with changes in EELV, from which changes in lung strain (7), alveolar recruitment (8) or dynamic hyperinflation (9) can be quantified;

(V) Quantification of global and regional perfusion: heart and lungs present out of phase impedance changes from which cardiac output (10), stroke volume variations, pulmonary artery pressure and global and regional lung perfusion can be quantified. Hypertonic saline boluses are usually implemented as tracer for magnification of the signal and increased accuracy (11);

(VI) Spatial heterogeneity of lung perfusion distribution: regional defect can be used to diagnose pulmonary embolism (12) while quantification of the regional heterogeneity could help stratification of acute respiratory failure severity, with higher heterogeneity associated with a higher risk of ventilation-induced lung injury.

© Journal of Emergency and Critical Care Medicine. All rights reserved.

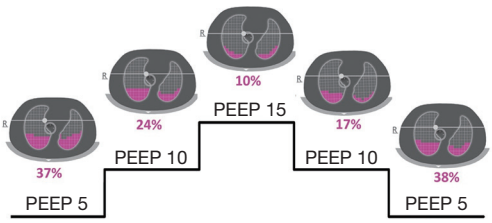

Figure 2 Lung recruitment and derecruitment. Representative EIT-derived "silent spaces" map of an ARDS patient during an incremental and decremental PEEP trial from PEEP 5 to 15 cmH_2O. Silent spaces, defined as pixels in the lung area (grey profiles) showing <10% tidal impedance change, are represented in pink. The grey circle represents the center of ventilation and the horizontal line passing through this point is used to divide the lung area into non-dependent (above the line) and dependent (below the line) parts. As shown, when increasing PEEP from 5 to 15 cmH_2O, dependent silent spaces decreased from 37% to 10% of the lung area (i.e., dorsal lung recruitment occurred). The opposite was observed when PEEP was decreased again to 5 cmH_2O (Authors' personal unpublished data). EIT, electrical impedance tomography; ARDS, acute respiratory distress syndrome; PEEP, positive end-expiratory pressure.

Respiratory monitoring

PEEP setting and recruitment

In patients with acute respiratory distress syndrome (ARDS), selection of an appropriate value of positive end-expiratory pressure (PEEP) is of cornerstone importance to maximize lung recruitment, reduce alveolar overdistension and avoid atelectrauma. Several studies have explored the possibility to guide the individual PEEP setting by EIT monitoring. Many EIT-derived indexes have been proposed, based on EIT capability to give regional information, e.g. separating dependent and non-dependent lung regions.

Costa *et al.* measured regional dynamic compliance (Pixel compliance = ΔZpixel/ΔPaw) during a decremental PEEP titration and found that the dependent lung regions progressively reduced their compliance, while the opposite was true for the non-dependent ones, suggesting the contemporary presence of two opposite phenomena: lung collapse and over-distension. Moreover, the Authors demonstrated a good correlation between EIT-derived and computed tomography-derived data (13). Another parameter that describes ventilation distribution is the GI index: the smaller its value, the more homogeneous is the distribution of ventilation. GI index has been shown to be comparable to dynamic compliance for determining the best PEEP during an incremental PEEP trial in patients with healthy lungs (14). Another EIT-derived index proposed to guide PEEP setting is the intratidal ventilation (ITV) index, applied in post cardiac surgery patients by Lowhagen *et al.* (15). This index measures the homogeneity of tidal volume distribution between the dependent and non-dependent regions and is as accurate as the dynamic compliance method in finding the best PEEP (16).

EIT allows to monitor EELV variations, which can be used to select the PEEP level needed to prevent derecruitment (17).

Furthermore, EIT is useful for assessing recruitment and regional distribution of ventilation during the open lung approach (18). EIT signal, combined with anthropometric parameters, can individuate poorly ventilated lung units, the so-called silent spaces, defined as regions exhibiting less than 10% of variations in impedance during tidal ventilation. The dynamic variation of dependent silent spaces during incremental and decremental PEEP steps correlates well with lung recruitment and derecruitment assessed by the pressure/volume (P/V) curve (3) (*Figure 2*).

Finally, EIT-guided PEEP selection has been studied during a decremental PEEP trial in patients undergoing extracorporeal membrane oxygenation. PEEP setting was ideally based on the balance between collapse and overdistension, i.e., the lowest PEEP level needed to limit the collapse to ≤15% with the least overdistension. This study showed a wide variability in optimal PEEP values, highlighting the need for individualized setting of mechanical ventilation (19).

Heterogeneity of ventilation distribution

The space and time resolution of EIT makes it an attractive tool to monitor fast changes in ventilation occurring at the alveolar (pixel) level, not easily captured by other available techniques. Conventional quantitative imaging of the thorax (CT scan) allows measuring volumes at end-expiration or end-inspiration in static conditions, which are almost never reached during tidal breathing. While the lung viscoelastic behavior has long been postulated by physiologists (20) and global airway pressure waveforms have been used to describe lung dynamic properties, no direct visualization of fast regional lung volume changes (21), redistribution of aeration (Pendelluft) or dynamic airflow limitation (22) was possible before EIT. It is thus not surprising that the number of EIT-derived indexes used to evaluate the heterogeneity

© Journal of Emergency and Critical Care Medicine. All rights reserved.

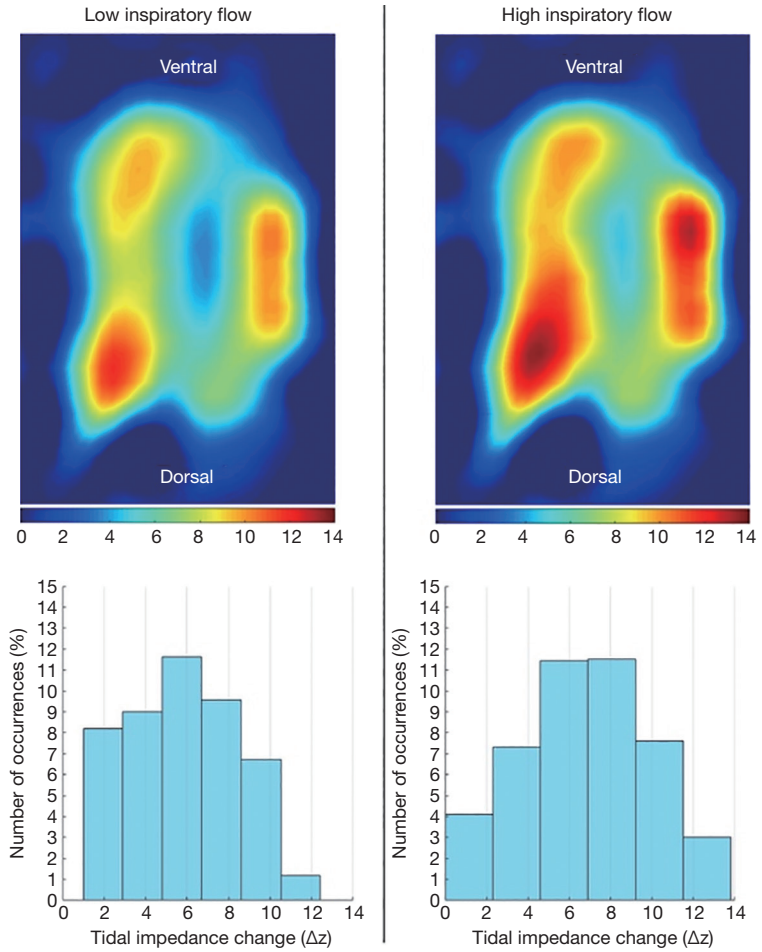

Figure 3 Heterogeneity of ventilation distribution. EIT images showing tidal volume distribution expressed in relative impedance units (upper panel) and histogram showing relative distribution of impedance (lower panel) in an ARDS patient ventilated with a tidal volume of 6 mL/kg of predicted body weight, delivered either with a low (400 mL/sec, left) or a high inspiratory flow (1,200 mL/sec, right). Higher inspiratory flow results in both higher impedance values, indicative or regional overdistention (red areas in the upper panel), and more spread distribution of impedance (i.e., ventilation) throughout the lungs (authors' personal unpublished data). EIT, electrical impedance tomography; ARDS, acute respiratory distress syndrome.

of ventilation keeps growing, given the importance of identifying the dynamic determinants of lung injury (23,24).

Heterogeneity is described in terms of (I) *amount* of ventilation at the pixel level at end inspiration, compared to the median ventilation of all pixels [GI index (5)]; (II) *fraction* of ventilation at the ROI level during different phases of inspiration [ITV distribution (15)]; (III) *rate* of inflation at the ROI or pixel level, compared to the global rate [filling index (25)]; (IV) *time* from start of ventilation in the whole EIT image to start of ventilation in the ROI or pixel [regional ventilation delay (26)] (*Table 1*).

Of note, while *aeration* heterogeneity has been demonstrated in ARDS patients (27), its role as an initiator/propagator of lung injury is indirect, requiring *ventilation* maldistribution in order to cause damage (4). The chance to measure even temporary occurrence of regional overinflation, which will disappear during redistribution in static conditions, and to monitor how different ventilator settings (e.g., respiratory rate, amount and shape of inspiratory flow) can affect these potentially dangerous transient states, is an invaluable tool for the treatment of ARDS (*Figure 3*).

© Journal of Emergency and Critical Care Medicine. All rights reserved.

Furthermore, inspiratory (and expiratory) ventilation heterogeneity, time constant inequalities and airflow limitation are typical features of chronic obstructive pulmonary disease (COPD) (28) and asthma (29). Severe acute exacerbations of these syndromes requiring mechanical ventilation are challenging and treatment could greatly benefit from EIT monitoring.

Spontaneous breathing

Spontaneous breathing is characterized by dynamic fluctuations of the respiratory pattern (e.g., sudden changes in tidal volume size and/or in the respiratory rate) and by limited accuracy of classic respiratory volume monitoring tools (e.g., spirometry can be performed only through a mouthpiece and closed nose altering the respiratory pattern, and static CT scan is simply not feasible). These characteristics make dynamic non-invasive EIT imaging the new gold standard for respiratory monitoring of lung volumes during spontaneous breathing. For example, in this era of rapidly spreading use of high flow nasal cannula (HFNC) in hypoxemic and hypercapnic patients (30,31), EIT could guide selection of a personalized HFNC flow rate (i.e. that associated with significant increase of EELV) (32) and it could be used to monitor changes in minute ventilation (33) or to detect potentially injurious (i.e., too large) tidal volumes (34). After intubation, early switch to assisted mechanical ventilation modes can be associated with strong inspiratory effort causing occult pendelluft of gas content from non-dependent to dependent lung region (35). EIT can quantify occult pendelluft and increased regional lung stretch, supporting interventions aimed at mitigating this phenomenon (e.g., increase PEEP level). Personalized pressure support level to avoid over- and under-assistance can also be inferred from optimized homogeneity assessed by EIT (36). Similarly, usefulness of new ventilation modes such as neurally adjusted ventilation assist (NAVA) or addition of Sigh to assisted ventilation (7) can be evaluated by EIT-derived variables such as improved homogeneity or increased EELV at constant PEEP (i.e., alveolar recruitment). Finally, during a spontaneous breathing trial, shift of the largest part of ventilation to the dependent lung region might indicate too strenuous inspiratory efforts and predict weaning failure, even in the presence of acceptable gas exchanges and respiratory rate.

Hemodynamic monitoring

Pulmonary perfusion and V/Q matching

Since cyclic variations in both pulmonary air and blood content are the major determinants for the changes in thoracic impedance, a logical application for EIT would be to combine imaging of lung perfusion with ventilation data to provide a global functional assessment of pulmonary gas exchange. To this end, cardiac-related impedance changes have been shown to reflect pulmonary blood content and are therefore a surrogate for pulmonary perfusion (37,38). However, perfusion imaging with EIT remains a challenge, both for technical difficulties and for the interpretation of the results. Perfusion impedance changes are much smaller than ventilation changes (39), complicating signal detection and filtering. Three different signal-processing techniques have been proposed to separate perfusion and ventilation components in EIT (38,40-42) but the best method remains to be defined because of lack of systematic comparison to standard perfusion imaging.

Whatever the method used, the amplitude of global EIT perfusion signal is related to the size of pulmonary vascular bed (43) and therefore can be used to assess anatomic and functional changes in pulmonary circulation. Indeed, clinical studies showed that EIT can document the loss of pulmonary vessels in COPD (44) and pulmonary artery hypertension (45), as well as changes in pulmonary vascular resistance (hypoxic vasoconstriction and hyperoxic vasodilation) (46).

Simultaneous perfusion and ventilation monitoring by EIT could allow dynamic assessment of ventilation/perfusion (V/Q) matching. In an experimental study on mechanically ventilated animals, global EIT V/Q ratio showed an acceptable correlation with calculated alveolar dead space and venous admixture during acute changes in pulmonary ventilation and perfusion (47). Grant *et al.* evaluated the ability of EIT to trace gravitational changes in the regional distribution of ventilation and perfusion in spontaneously breathing subjects; they reported the potential limits of EIT-derived regional V/Q ratio, mainly due to the use of relative changes of ventilation and perfusion impedance instead of absolute values (38). To overcome this and other issues related to the interpretation of cardiac-related impedance changes as surrogate for pulmonary perfusion, Borges *et al.* proposed an EIT-based

© Journal of Emergency and Critical Care Medicine. All rights reserved.

method that quantitatively estimates regional lung perfusion based on first-pass kinetics of a bolus of hypertonic saline contrast (11). Accuracy is improved by this technique, providing reliable measurement of regional blood flow in healthy lungs and in experimental models of alveolar collapse (11) and pulmonary embolism (37). Nevertheless, the use of large quantities of this hypertonic solution (20% sodium chloride) represents a major limitation to the clinical applicability of this technique.

Cardiac output and fluid responsiveness

Cardiac-related changes in thoracic impedance can also be used for non-invasive hemodynamic monitoring. As these changes are caused by the passage of the stroke volume through the lungs, a strong correlation has been found between their amplitude and stroke volume measured by thermodilution (10), supporting the use of EIT for dynamic cardiac monitoring. Moreover, EIT might be used to predict fluid responsiveness by providing non-invasive evaluation of stroke volume variations inside the aorta, which correlate well with the same index assessed by aortic ultrasonic flow probe and from arterial pulse contour analysis, both in healthy animals (48) and in experimental lung injury (49).

Non-invasive dynamic monitoring of pulmonary and central hemodynamics is a novel promising application of EIT, but current knowledge is mostly based on animal models and confirmation in clinical studies is mandatory prior to clinical use. Although based on the same physiologic principles, EIT indexes are intrinsically different from the "standard" comparators, because EIT parameters derive from relative impedance changes. Understanding the underlying assumptions is key to their correct interpretation.

Pediatric patients

Children, while being undoubtedly smaller than adults, are not small adults. Furthermore, it is worth underlining that the lungs develop and grow, as does the child. Indeed, both the number of alveoli and their size increase over time. Alveoli increase in number, over tenfold from birth to adult life, while alveolar diameter increases slightly in the first 8 years of life, thereafter reaching a value similar to that of adults (50,51). Finally, newborns present a high percentage of lung tissue, mainly localized at the points of bifurcation of alveolar ducts and respiratory bronchioles (50). However, the percentage of lung tissue decreases with age, leading, in combination with the increase in alveolar number and size, to a reduction in lung density (52) and therefore to an increase in impedance (53). The discussed dynamicity of young lungs, in combination with the difficulties in obtaining reliable/repeated physiologic measurements and the logical attempt to reduce/avoid radiation exposure in this highly radiosensitive population, make thoracic EIT particularly interesting for pediatric critical care physicians. In addition, the smaller size of children's lungs allows the assessment, with EIT, of a greater part of the parenchyma, as compared to adults.

Several studies investigating the use of EIT have been conducted in the pediatric intensive care unit. The feasibility of EIT monitoring in pediatric patients was first demonstrated by Frerichs and colleagues in eight critically ill children requiring intensive care treatment for various diseases (54). Thereafter, Wolf *et al.* used EIT to describe regional lung volume changes occurring during airway suctioning in children with ARDS (55). The same group used EIT to describe the regional dynamics of lung reopening and overdistension during the performance of a recruitment maneuver in critically ill children with acute lung injury (56). Another recent study evaluated with EIT the effect of prone positioning in children with ARDS, showing an improvement in lung homogeneity and recruitment of the dorsal lung regions (57).

In summary, EIT seems a very promising technique to evaluate and monitor global and regional lung function. It could be particularly interesting and useful in the pediatric population, where the avoidance of radiation exposure is of paramount importance.

The discussion of the use of thoracic EIT in the Neonatal ICU is beyond the scope of the present review.

Perioperative monitoring

Reports describing EIT use during general anesthesia for surgery are growing in number in recent years. Most of the current use is for monitoring derecruitment and PEEP setting in obese patients, especially in the setting of laparoscopic surgery (58-60). Another field of interest, for obvious reasons, is thoracic surgery. Reliable evaluation of correct exclusion of one side for one-lung ventilation is made possible by EIT (61,62). A major limitation of this technique during surgery regards belt position interference with the surgical field: while feasibility of intraoperative monitoring during upper abdominal surgery has been

© Journal of Emergency and Critical Care Medicine. All rights reserved.

shown (63), evaluations during thoracic surgery can be performed only before the start or after the end of the operation.

Pediatric anesthesia and surgery merit a separated mention. The already discussed advantages for pediatric patients (small lung size, radiation-free technique) make EIT a valuable monitoring tool. Indeed, EIT has been employed to assess intratidal recruitment/derecruitment and the effect of PEEP in 39 children undergoing elective ear, nose and throat surgery (64). Furthermore, EIT could be a useful tool to evaluate the correct placement of endotracheal tubes (65).

Other less common applications of EIT in the operating room such as evaluation of complete recovery of ventilation after paralysis reversal (66) and hemi diaphragmatic paresis after locoregional anesthesia (67) have been occasionally reported.

Future applications

EIT is just at its dawn. We have described the principal fields of current clinical use, but the growing number of innovative applications being reported (68) confirms the increasing interest of clinicians for this informative, easy to apply technique.

We can expect EIT to be increasingly employed in ARDS patients, to unveil what has thus far been just inferred from CT scan analysis, without being possible to record it "live": opening and closing phenomena (3), pendelluft (35), dynamic overdistention (9). Even if EIT, as any other monitoring tool, cannot improve outcome *per se*, the knowledge of the dynamic pathophysiology of the patient, derived from EIT, can be used to take clinical decisions and tailor treatment. Future studies will address if clinical management based on EIT-derived parameters, such as alveolar recruitment and lung heterogeneity, can reduce mortality, or other clinically relevant outcomes, of ARDS patients.

Diseases characterized by heterogeneity of ventilation distribution such as pediatric and adult asthma, bronchiolitis and adult COPD will surely benefit from a monitoring tool able to measure and display inflation and deflation (69) patterns of fast and slow pulmonary units (i.e., measuring time constants) (70,71).

Hemodynamic monitoring lags some steps behind respiratory monitoring but is currently receiving a great interest both in the ICU and in the operating room, since cardiac output measurement and fluid responsiveness are cornerstones of the care of the critically-ill patient.

Finally, the application of the EIT belt to awake or anesthetized spontaneously breathing subjects will probably spread its use outside the intensive care and anesthesia settings. Pulmonologists have already started using it for pulmonary function testing (72,73), and us as intensivists should not underestimate the advantages of portability, expanding the use EIT to the pre-anesthesia outpatient clinic (e.g., before thoracic surgery) and for monitoring in non-operating room anesthesia settings (74).

Conclusions

EIT has just entered our intensive care units and operating rooms. Its non-invasiveness and the unique capability of dynamically assessing the function of intrathoracic organs, make it a perfect candidate for monitoring of critically-ill patients, and will probably change our clinical practice in the next few years. We should welcome this change, to improve patients' safety and our ability to tailor treatments to specific patient's need.

Acknowledgements

None.

Footnote

Conflicts of Interest: G Grasselli received payment for lectures from Getinge, Draeger Medical, Fisher & Paykel, Pfizer; G Grasselli received support for travel/congresses from Getinge and Biotest. T Mauri received personal fees for lectures from Drager outside of the present work. The other authors have no conflicts of interest to declare.

References

1. Hahn G, Frerichs I, Kleyer M, et al. Local mechanics of the lung tissue determined by functional EIT. Physiol Meas 1996;17 Suppl 4A:A159-66.
2. Victorino JA, Borges JB, Okamoto VN, et al. Imbalances in regional lung ventilation. Am J Respir Crit Care Med 2004;169:791-800.
3. Spadaro S, Mauri T, Böhm SH, et al. Variation of poorly ventilated lung units (silent spaces) measured by electrical impedance tomography to dynamically assess recruitment. Crit Care 2018;22:26.
4. Mead J, Takishima T, Leith D. Stress distribution in lungs: a model of pulmonary elasticity. J Appl Physiol

© Journal of Emergency and Critical Care Medicine. All rights reserved.

1970;28:596-608.
5. Zhao Z, Möller K, Steinmann D, et al. Evaluation of an electrical impedance tomography-based global inhomogeneity index for pulmonary ventilation distribution. Intensive Care Med 2009;35:1900-6.
6. Wolf GK, Gómez-Laberge C, Rettig JS, et al. Mechanical ventilation guided by electrical impedance tomography in experimental acute lung injury. Crit Care Med 2013;41:1296-304.
7. Mauri T, Eronia N, Abbruzzese C, et al. Effects of sigh on regional lung strain and ventilation heterogeneity in acute respiratory failure patients undergoing assisted mechanical ventilation. Crit Care Med 2015;43:1823-31.
8. Mauri T, Eronia N, Turrini C, et al. Bedside assessment of the effects of positive end-expiratory pressure on lung inflation and recruitment by the helium dilution technique and electrical impedance tomography. Intensive Care Med 2016;42:1576-87.
9. Adler A, Shinozuka N, Berthiaume Y, et al. Electrical impedance tomography can monitor dynamic hyperinflation in dogs. J Appl Physiol 1998 Feb;84:726-32.
10. Vonk-Noordegraaf A, Janse A, Marcus JT, et al. Determination of stroke volume by means of electrical impedance tomography. Physiol Meas 2000;21:285-93.
11. Borges JB, Suarez-Sipmann F, Böhm SH, et al. Regional lung perfusion estimated by electrical impedance tomography in a piglet model of lung collapse. J Appl Physiol 2012;112:225-36.
12. Nguyen DT, Bhaskaran A, Chik W, et al. Perfusion redistribution after a pulmonary-embolism-like event with contrast enhanced EIT. Physiol Meas 2015;36:1297-309.
13. Costa EL, Borges JB, Melo A, et al. Bedside estimation of recruitable alveolar collapse and hyperdistension by electrical impedance tomography. Intensive Care Med 2009;35:1132-7.
14. Zhao Z, Steinmann D, Frerichs I, et al. PEEP titration guided by ventilation homogeneity: a feasibility study using electrical impedance tomography. Crit Care 2010;14:R8.
15. Lowhagen K, Lundin S, Stenqvist O. Regional intratidal gas distribution in acute lung injury and acute respiratory distress syndrome assessed by electric impedance tomography. Minerva Anestesiol 2010;76:1024-35.
16. Blankman P, Hasan D, Erik G, et al. Detection of "best" positive end-expiratory pressure derived from electrical impedance tomography parameters during a decremental positive end-expiratory pressure trial. Crit Care 2014;18:R95.
17. Eronia N, Mauri T, Maffezzini E, et al. Bedside selection of positive end-expiratory pressure by electrical impedance tomography in hypoxemic patients: a feasibility study. Ann Intensive Care 2017;7:76.
18. Cinnella G, Grasso S, Raimondo P, et al. Physiological effects of the open lung approach in patients with early, mild, diffuse Acute Respiratory Distress Syndrome: an electrical impedance tomography study. Anesthesiology 2015;123:1113-21.
19. Franchineau G, Bréchot N, Lebreton G, et al. Bedside contribution of electrical impedance tomography to setting positive end-expiratory pressure for extracorporeal membrane oxygenation-treated patients with severe Acute Respiratory Distress Syndrome. Am J Respir Crit Care Med 2017;196:447-57.
20. Otis AB, McKerrow CB, Bartlett RA, et al. Mechanical factors in distribution of pulmonary ventilation. J Appl Physiol 1956;8:427-43.
21. Georgopoulos D, Mitrouska I, Markopoulou K, et al. Effects of breathing patterns on mechanically ventilated patients with chronic obstructive pulmonary disease and dynamic hyperinflation. Intensive Care Med 1995;21:880-6.
22. Pankow W, Podszus T, Gutheil T, et al. Expiratory flow limitation and intrinsic positive end-expiratory pressure in obesity. J Appl Physiol 1998;85:1236-43.
23. Protti A, Maraffi T, Milesi M, et al. Role of strain rate in the pathogenesis of ventilator-induced lung edema. Crit Care Med 2016;44:e838-45.
24. Gattinoni L, Tonetti T, Cressoni M, et al. Ventilator-related causes of lung injury: the mechanical power. Intensive Care Med 2016;42:1567-75.
25. Grant CA, Fraser JF, Dunster KR, et al. The assessment of regional lung mechanics with electrical impedance tomography: a pilot study during recruitment manoeuvres. Intensive Care Med 2009;35:166-70.
26. Wrigge H, Zinserling J, Muders T, et al. Electrical impedance tomography compared with thoracic computed tomography during a slow inflation maneuver in experimental models of lung injury. Crit Care Med 2008;36:903-9.
27. Cressoni M, Cadringher P, Chiurazzi C, et al. Lung inhomogeneity in patients with Acute Respiratory Distress Syndrome. Am J Respir Crit Care Med 2014;189:149-58.
28. Farré R, Ferrer M, Rotger M, et al. Respiratory mechanics in ventilated COPD patients: forced oscillation versus occlusion techniques. Eur Respir J 1998;12:170-6.
29. Aysola R, de Lange EE, Castro M, et al. Demonstration of the heterogeneous distribution of asthma in the lungs using CT and hyperpolarized helium-3 MRI. J Magn

© Journal of Emergency and Critical Care Medicine. All rights reserved.

Reson Imaging 2010;32:1379-87.
30. Mauri T, Turrini C, Eronia N, et al. Physiologic effects of high-flow nasal cannula in acute hypoxemic respiratory failure. Am J Respir Crit Care Med 2017;195:1207-15.
31. Di Mussi R, Spadaro S, Stripoli T, et al. High-flow nasal cannula oxygen therapy decreases postextubation neuroventilatory drive and work of breathing in patients with chronic obstructive pulmonary disease. Crit Care 2018;22:180.
32. Corley A, Caruana LR, Barnett AG, et al. Oxygen delivery through high-flow nasal cannulae increase end-expiratory lung volume and reduce respiratory rate in post-cardiac surgical patients. British Journal of Anaesthesia. Br J Anaesth 2011;107:998-1004.
33. Mauri T, Alban L, Turrini C, et al. Optimum support by high-flow nasal cannula in acute hypoxemic respiratory failure: effects of increasing flow rates. Intensive Care Med 2017;43:1453-63.
34. Brochard L, Slutsky A, Pesenti A. Mechanical ventilation to minimize progression of lung injury in acute respiratory failure. Am J Respir Crit Care Med 2017;195:438-42.
35. Yoshida T, Torsani V, Gomes S, et al. Spontaneous effort causes occult Pendelluft during mechanical ventilation. Am J Respir Crit Care Med 2013;188:1420-7.
36. Mauri T, Lazzeri M, Bronco A, et al. Effects of variable pressure support ventilation on regional homogeneity and aeration. Am J Respir Crit Care Med 2017;195:e27-8.
37. Frerichs I, Hinz J, Herrmann P, et al. Regional lung perfusion as determined by electrical impedance tomography in comparison with electron beam CT imaging. IEEE Trans Med Imaging 2002;21:646-52.
38. Grant CA, Pham T, Hough J, et al. Measurement of ventilation and cardiac related impedance changes with electrical impedance tomography. Crit Care 2011;15:R37.
39. Eyuboglu BM, Brown BH, Barber DC. In vivo imaging of cardiac related impedance changes. IEEE Eng Med Biol Mag 1989;8:39-45.
40. McArdle FJ, Suggett AJ, Brown BH, et al. An assessment of dynamic images by applied potential tomography for monitoring pulmonary perfusion. Clin Phys Physiol Meas 1988;9 Suppl A:87-91.
41. Frerichs I, Pulletz S, Elke G, et al. Assessment of changes in distribution of lung perfusion by electrical impedance tomography. Respiration 2009;77:282-91.
42. Deibele JM, Luepschen H, Leonhardt S. Dynamic separation of pulmonary and cardiac changes in electrical impedance tomography. Physiol Meas 2008;29:S1-S14.
43. Smit HJ, Vonk-Noordegraaf A, Marcus JT, et al. Determinants of pulmonary perfusion measured by electrical impedance tomography. Eur J Appl Physiol 2004;92:45-9.
44. Vonk Noordegraaf A, Kunst PW, Janse A, et al. Pulmonary perfusion measured by means of electrical impedance tomography. Physiol Meas 1998;19:263-73.
45. Smit HJ, Vonk Noordegraaf A, Boonstra A, et al. Assessment of the pulmonary volume pulse in idiopathic pulmonary arterial hypertension by means of electrical impedance tomography. Respiration 2006;73:597-602.
46. Smit HJ, Vonk-Noordegraaf A, Marcus J, et al. Pulmonary vascular responses to hypoxia and hyperoxia in healthy volunteers and COPD patients measured by electrical impedance tomography. Chest 2003;123:1803-9.
47. Fagerberg A, Stenqvist O, Åneman A. Electrical impedance tomography applied to assess matching of pulmonary ventilation and perfusion in a porcine experimental model. Crit Care 2009;13:R34.
48. Maisch S, Böhm SH, Solà J, et al. Heart-lung interactions measured by electrical impedance tomography. Crit Care Med 2011;39:2173-6.
49. Trepte CJC, Phillips C, Solà J, et al. Electrical impedance tomography for non-invasive assessment of stroke volume variation in health and experimental lung injury. Br J Anaesth 2017;118:68-76.
50. Dunnill MS. Quantitative methods in the study of pulmonary pathology. Thorax 1962;17:320-8.
51. Narayanan M, Owers-Bradley J, Beardsmore CS, et al. Alveolarization continues during childhood and adolescence. Am J Respir Crit Care Med 2012;185:186-91.
52. Stein JM, Walkup LL, Brody AS, et al. Quantitative CT characterization of pediatric lung development using routine clinical imaging. Pediatr Radiol 2016;46:1804-12.
53. Brown BH, Primhak RA, Smallwood RH, et al. Neonatal lungs--can absolute lung resistivity be determined non-invasively? Med Biol Eng Comput 2002;40:388-94.
54. Frerichs I, Schiffmann H, Hahn G, et al. Non-invasive radiation-free monitoring of regional lung ventilation in critically ill infants. Intensive Care Med 2001;27:1385-94.
55. Wolf GK, Grychtol B, Frerichs I, et al. Regional lung volume changes in children with acute respiratory distress syndrome during a derecruitment maneuver. Crit Care Med 2007;35:1972-8.
56. Wolf GK, Gómez-Laberge C, Kheir JN, et al. Reversal of dependent lung collapse predicts response to lung recruitment in children with early acute lung injury. Pediatr Crit Care Med 2012;13:509-15.

© Journal of Emergency and Critical Care Medicine. All rights reserved.

57. Lupton-Smith A, Argent A, Rimensberger P, et al. Prone positioning improves ventilation homogeneity in children with Acute Respiratory Distress Syndrome. Pediatr Crit Care Med 2017;18:e229-34.
58. Karsten J, Luepschen H, Grossherr M, et al. Effect of PEEP on regional ventilation during laparoscopic surgery monitored by electrical impedance tomography. Acta Anaesthesiol Scand 2011;55:878-86.
59. Erlandsson K, Odenstedt H, Lundin S, et al. Positive end-expiratory pressure optimization using electric impedance tomography in morbidly obese patients during laparoscopic gastric bypass surgery. Acta Anaesthesiol Scand 2006;50:833-9.
60. Stankiewicz-Rudnicki M, Gaszynski W, Gaszynski T. Assessment of ventilation distribution during laparoscopic bariatric surgery: an electrical impedance tomography study. Biomed Res Int 2016;2016:7423162.
61. Steinmann D, Stahl CA, Minner J, et al. Electrical impedance tomography to confirm correct placement of double-lumen tube: a feasibility study. Br J Anaesth 2008;101:411-8.
62. Pulletz S, Elke G, Zick G, et al. Performance of electrical impedance tomography in detecting regional tidal volumes during one-lung ventilation. Acta Anaesthesiol Scand 2008;52:1131-9.
63. Schaefer MS, Wania V, Bastin B, et al. Electrical impedance tomography during major open upper abdominal surgery: a pilot-study. BMC Anesthesiol 2014;14:51.
64. Wirth S, Artner L, Broß T, et al. Intratidal recruitment/derecruitment persists at low and moderate positive end-expiratory pressure in paediatric patients. Respir Physiol Neurobiol 2016;234:9-13.
65. Steinmann D, Engehausen M, Stiller B, et al. Electrical impedance tomography for verification of correct endotracheal tube placement in paediatric patients: a feasibility study. Acta Anaesthesiol Scand 2013;57:881-7.
66. Carron M, Galzignato C, Godi I, et al. Benefit of sugammadex on lung ventilation evaluated with electrical impedance tomography in a morbidly obese patient undergoing bariatric surgery. J Clin Anesth 2016;31:78-9.
67. Wiegel M, Hammermüller S, Wrigge H, et al. Electrical impedance tomography visualizes impaired ventilation due to hemidiaphragmatic paresis after interscalene brachial plexus block. Anesthesiology 2016;125:807.
68. Guérin C, Frerichs I. Getting a better picture of the correlation between lung function and structure using electrical impedance tomography. Am J Respir Crit Care Med. 2014;190:1186-7.
69. Mauri T, Bellani G, Salerno D, et al. Regional distribution of air trapping in chronic obstructive pulmonary disease. Am J Respir Crit Care Med 2013;188:1466-7.
70. Miedema M, de Jongh FH, Frerichs I, et al. Regional respiratory time constants during lung recruitment in high-frequency oscillatory ventilated preterm infants. Intensive Care Med 2012;38:294-9.
71. de la Oliva P, Waldmann AD, Böhm SH, et al. Bedside breath-wise visualization of bronchospasm by electrical impedance tomography could improve perioperative patient safety. A A Case Rep 2017;8:316-9.
72. Vogt B, Pulletz S, Elke G, et al. Spatial and temporal heterogeneity of regional lung ventilation determined by electrical impedance tomography during pulmonary function testing. J Appl Physiol 2012;113:1154-61.
73. Frerichs I, Zhao Z, Becher T, et al. Regional lung function determined by electrical impedance tomography during bronchodilator reversibility testing in patients with asthma. Physiol Meas 2016;37:698-712.
74. Bordes J, Goutorbe P, Cungi PJ, et al. Noninvasive ventilation during spontaneous breathing anesthesia: an observational study using electrical impedance tomography. J Clin Anesth 2016;34:420-6.

doi: 10.21037/jeccm.2018.08.08
Cite this article as: Santini A, Spinelli E, Langer T, Spadaro S, Grasselli G, Mauri T. Thoracic electrical impedance tomography: an adaptive monitor for dynamic organs. J Emerg Crit Care Med 2018;2:71.

© Journal of Emergency and Critical Care Medicine. All rights reserved.